

Accumulation of 2-Deoxy-2-[¹⁸F]Fluoro-D-Glucose in Human Cancers Heterotransplanted in Nude Mice: Comparison Between Histology and Glycolytic Status

Takashi Yoshioka, Hiromu Takahashi, Hirosuke Oikawa, Syunichi Maeda, Akira Wakui, Tadashi Watanabe, Fumiaki Tezuka, Tohru Takahashi, Tatuo Ido and Ryunosuke Kanamaru

Department of Clinical Oncology, Department of Pathology, Institute of Development, Aging and Cancer, and Cyclotron and Radioisotope Center, Tohoku University, Sendai, Japan

The success of tumor imaging with PET and 2-deoxy-2-fluoro[¹⁸F]-D-glucose (¹⁸FDG) is based on preferential accumulation of ¹⁸FDG in tumors. **Methods:** Fluorine-18-FDG uptake was measured in nine human cancers heterotransplanted in nude mice and compared with histologic subclassification. **Results:** Mean ¹⁸FDG uptake by the human cancers was considerably less than that by the host's heart, but values at 60 min after injection were about 2.5 times as high as the liver and kidney, about two times as that for the muscle and about six times that for the blood. Comparison of ¹⁸FDG uptake and histological grade in four gastric, two pancreatic and three colonic cancers showed that ¹⁸FDG uptake increased with loss of differentiation. **Conclusion:** This nude mice model system is useful for studying correlations between physiological and morphological parameters of heterotransplanted human cancers.

Key Words: fluorine-18-2DG deoxyglucose; nude mice; human cancer

J Nucl Med 1994; 35:97-103

Increased glycolysis is one of the most important characteristics of cancer cells (1-4). Fluorine-18-2-deoxy-2-fluoro-D-glucose (¹⁸FDG), a structural analog like glucose, labeled with the short-lived positron-emitting radioisotope ¹⁸F, is transported across the cell membrane and converted into ¹⁸FDG-6-PO₄ by hexokinase within cells (5,6). However, because ¹⁸FDG-6-PO₄ is not a substrate for further metabolism, it is trapped in the cells (7,8), which facilitates the use of positron emission tomography (PET), a technique which allows reconstruction of transaxial tomographic images of the distribution of positron-emitting ra-

diopharmaceuticals in the human head and torso (9). Because ¹⁸FDG is preferentially taken up by malignant tumors in accordance with their increased glycolysis, PET with ¹⁸FDG as a radiopharmaceutical makes it possible to obtain clinical images of malignant tumors (10-15).

Several clinical PET studies (10-15) and experiments using animal tumor models (16-18) have confirmed that ¹⁸FDG accumulates in malignant tumors. However, little information is available on its relationship to human tumor biology. In this study, we investigated ¹⁸FDG accumulation into human cancer tissues heterotransplanted in nude mice as a model system.

Weber and other investigators observed a correlation between histologic subclassification and glycolytic rate in rat hepatomas (3,4,19-23). They observed that the transformation from slow-growing, well differentiated tumors to rapidly growing, poorly differentiated lesions was accompanied by a progressive increase in glycolysis. Evidence for this from human cancers, however, is limited. The present study took advantage of the fact that the accumulation rate of ¹⁸FDG reflects utilization of exogenous glucose (7). The aim was to determine whether accumulation of ¹⁸FDG in tumor tissues correlates with histologic subclassification and thereby contributes to the clinical analysis of ¹⁸FDG-PET tumor images. For this purpose, ¹⁸FDG accumulation rates were measured in nine human cancers, including four gastric, two pancreatic and three colonic carcinomas, heterotransplanted into nude mice.

MATERIALS AND METHODS

Animals

Inbred 4-wk-old male BALB/c nu/nu nude mice weighing 16-18 g were maintained under pathogen-free conditions for 1 wk prior to the study. They were given sterile food and water ad libitum. Five-week-old mice weighing 18-20 g were used for heterotransplantation.

Received Apr. 30, 1993; revision accepted Sept. 28, 1993.

For correspondence or reprints contact: Takashi Yoshioka, MD, Department of Clinical Oncology, Institute of Development, Aging and Cancer, Tohoku University, 4-1, Seiryomachi, Aoba-ku, Sendai, 980, Japan (Tel 022-274-1111 ext. 3445).

Tumors

Nine human cancers were investigated, including four gastric cancers, H-111, NS-8, SC-6-JCK and SH-10; two pancreatic cancers, PAN-1-RITC and PAN-2-RITC; and three colonic cancers, WiDr, SCC, and CoLo 205 (CoLo).

The tumor lines were established as follows: H-111, Department of Oncology Surgery, Research Institute for Microbiological Disease, Osaka University (24); NS-8, 1st Department of Surgery, Nara Medical University (25); SC-6-JCK, Central Institute for Experimental Animals (24); SH-10, Department of Surgery, Research Institute for Nuclear Medicine and Biology, Hiroshima University (26); and SCC, Department of Surgery, Cancer Research Institute, Kanazawa University (27). These cancers were kindly supplied by the respective laboratories and serially transplanted to nude mice at our institution. Third to fifth-generation transplants were investigated.

In addition, *in vitro* cell lines, WiDr, established at Lederle Laboratories in 1971 (28), and CoLo, established at Denver General Hospital in 1975 (29), were kindly supplied by Zenyaku Co., Ltd., and Otsuka Pharmaceutical Co., Ltd., respectively. After serial transplantation to nude mice at our institution, the third-generation transplants were used in this study.

PAN-1-RITC and PAN-2-RITC were established and maintained at our institution (30). The ninth-generation transplants were examined in this study.

Radio pharmaceutical

Fluorine-18-2-deoxy-2-fluoro-D-glucose (^{18}F FDG) was synthesized by the method described by Shiue (31). The specific activity varied according to the integrated cyclotron beam dose on the target and ranged from 1 to 10 mCi/mg at the end of synthesis. Radiochemical purity was 97%–98%.

Tumor Inoculation and Measurement of Tumor Size

Tumor tissue fragments, approximately 2 mm² in size, were inoculated into the subcutaneous tissue of the back of 5-wk-old nude mice (18–20 g body weight) under ether anesthesia with a trocar needle. Tumors were measured (length and width) with sliding calipers three times per week by the same person for 3–4 wk post-transplantation before studies of ^{18}F FDG tissue distribution were commenced. Tumor weights in milligrams were calculated according to the method of Geran et al. (32) from linear measurements using the formula:

$$\text{tumor weight (mg)} = \text{length (mm)} \times (\text{width (mm)})^2/2.$$

Growth curves were generated from the calculated tumor weights and tumor doubling times were calculated from the curves.

Fluorine-18-FDG Tissue Distribution Study

At 3–4 wk post-transplantation, the mice developed tumors that were 1–1.5 cm in diameter. Fluorine-18-FDG was dissolved in isotonic saline and the injected dose, approximately 15 $\mu\text{Ci}/0.2\text{ ml}$, was injected intravenously via the lateral tail vein. The mice were killed by decapitation, and exsanguinated at 10, 30, 60 or 90 min after injection, at which times blood samples were collected. Five to six mice were studied per group. The tumors and major organs (heart, liver, kidney, muscle) were removed and blotted. Blood and tissues were weighed and counted in an automated NaI well counter along with a standard sample of the injected dose (United Technologies Packard Auto-Gamma 500/800). Radioactivity was corrected for decay. Data were expressed as the percentage of the

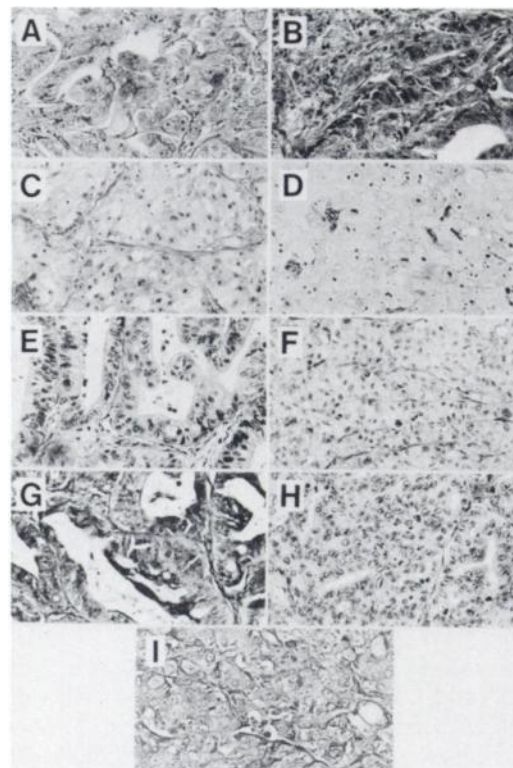


FIGURE 1. Histology of nine human cancers ($\times 200$). (A) H-111 (well differentiated gastric adenocarcinoma). (B) NS-8 (moderately differentiated gastric adenocarcinoma). (C) SC-6-JCK (poorly differentiated gastric carcinoma). (D) SH-10 (undifferentiated gastric carcinoma). (E) PAN-1-RITC (well differentiated pancreatic adenocarcinoma). (F) PAN-2-RITC (poorly differentiated pancreatic adenocarcinoma). (G) WiDr (well differentiated colonic adenocarcinoma). (H) SCC (moderately differentiated colonic adenocarcinoma). (I) CoLo (poorly differentiated colonic adenocarcinoma).

injected dose per gram of tumor or organ (%ID/g tissue). Tumor-to-blood ratios were also calculated from %ID/g tissue values.

Histologic Examination and Measurement of Tumor Parenchyma-to-Stroma Volume Ratio

After radioactivity counting, residual tumor material was fixed in 10% aqueous formal saline, embedded in paraffin and cut to give cross-sections of the maximum area. Two sections of each tumor were prepared and mounted on slides. One was stained with hematoxylin and eosin and processed for histologic subclassification by pathologists. The other was stained with elastica and Masson's and processed for measuring the volume ratio of tumor parenchyma-to-stroma by the point counting method previously described by Weidel (33). One hundred fifty points per slide were counted on 10 slides for each cancer type for mean volume ratios of tumor parenchyma to stroma.

RESULTS

Histologic Examination

Histologic subclassification of the nine human cancers was made using hematoxylin and eosin stained slides. Representative histologic pictures are shown in Figure 1. H-111 (Fig. 1A) is a well differentiated gastric adenocarcinoma with a distinct glandular structure comprised of many cylindrical to cuboidal carcinoma cells arranged in single

layers. NS-8 (Fig. 1B) is a moderately differentiated gastric adenocarcinoma showing irregular, incomplete glandular structures and areas of solid medullary patterns. SC-6-JCK (Fig. 1C) is a poorly differentiated gastric adenocarcinoma predominantly comprised of solid medullary structures with a small number of areas of microglands. SH-10 (Fig. 1D) is an undifferentiated gastric carcinoma with no glandular elements. PAN-1-RITC (Fig. 1E) is a well differentiated pancreatic adenocarcinoma with distinct glandular structures. PAN-2-RITC (Fig. 1F) is a poorly differentiated pancreatic adenocarcinoma with mixed glandular and solid medullary structures, with cells arranged in cords. WiDr (Fig. 1G) is a well differentiated colonic adenocarcinoma with distinct glandular structures; the carcinoma cells are arranged in single layers. SCC (Fig. 1H) is a moderately differentiated colonic adenocarcinoma demonstrating mixed glandular and solid medullary areas. CoLo (Fig. 1I) is a poorly differentiated colonic adenocarcinoma composed of solid medullary structures, but it also demonstrates intracytoplasmic lumens often seen in adenocarcinomas.

Tumor Parenchyma-to-Stroma Volume Ratios

Volume ratios of tumor parenchyma-to-stroma for the nine human cancers were: H-111 3.9, NS-8 4.0, SC-6-JCK 3.9, SH-10 4.1, PAN-1-RITC 4.2, PAN-2-RITC 4.1, WiDr 4.1, SCC 3.8 and CoLo 4.0. There were no statistically significant differences between tumor parenchyma-to-stroma volume ratios in the various tumors studied.

Tumor Growth Curves

Tumors growth curves, which were calculated by the method of Geran et al. (32) are shown in Figure 2. All four gastric cancers demonstrated similar curves (Fig. 2A). The two pancreatic cancers also grew at essentially the same rates (Fig. 2B), as did the moderately and poorly differentiated colonic adenocarcinomas (Fig. 2C). The only linked difference in tumor growth was observed for the well differentiated colonic adenocarcinoma, which grew more slowly than the other two colonic neoplasms (Fig. 2C).

Tumor doubling times (days) of the four gastric cancers were as follows: H-111 (well differentiated adenocarcinoma) 5.4 ± 1.2 , NS-8 (moderately differentiated adenocarcinoma) 5.0 ± 1.0 , SC-6-JCK (poorly differentiated adenocarcinoma) 5.1 ± 0.9 , SH-10 (undifferentiated carcinoma) 5.1 ± 1.0 . There were no statistically significant differences between tumor growth rate. Similarly, for the two pancreatic cancers no difference was found: PAN-1-RITC (well differentiated adenocarcinoma) 11.7 ± 2.4 , PAN-2-RITC (poorly differentiated adenocarcinoma) 11.7 ± 4.5 . For the three colonic cancers, WiDr (well differentiated adenocarcinoma) 7.0 ± 2.4 , SCC (moderately differentiated adenocarcinoma) 3.1 ± 0.3 , and CoLo (poorly differentiated adenocarcinoma) 3.9 ± 0.6 , a statistically significant difference was evident between the well differentiated and two other types of adenocarcinomas ($p < 0.01$).

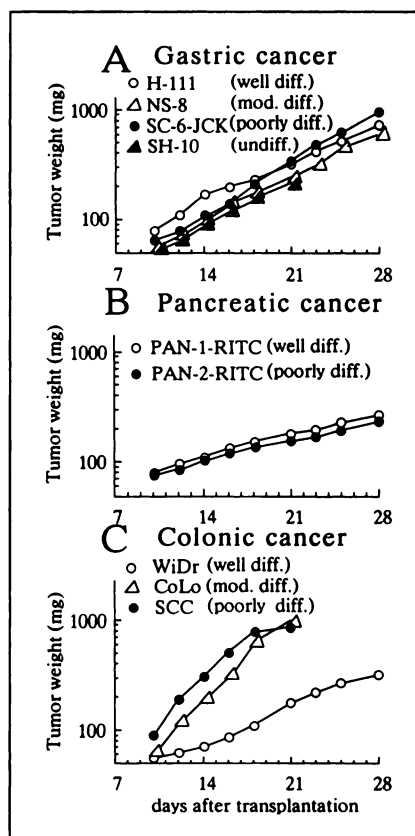


FIGURE 2. Tumor growth curves. The curves of four gastric cancers as well as two pancreatic cancers are similar. Only the well differentiated colonic adenocarcinoma grew more slowly than the other two colonic cancers. Dots indicate mean value.

Fluorine-18-FDG Tissue Distribution

Tissue distribution data of ^{18}F FDG in nude mice at 10, 30, 60 and 90 min after injection are summarized in Table 1. Uptake was greatest in each cancer cell line followed by the heart and muscles; uptake values remained relatively constant between the 30- and 90-min time points. Heart and muscle levels also remained relatively constant between 10 and 90 min, but clearance from the kidneys, liver and blood was very rapid (Fig. 3). The mean value of ^{18}F FDG uptake by the human cancers at 60 min after injection was about 2.5 times higher than that by the liver and kidneys, about two times higher than that by the muscle and about six times higher than by blood.

Comparative tumor uptake data for the cancers at 60 min after administration of ^{18}F FDG are summarized in Figure 4. Differences between H-111 and the three other gastric cancers and between NS-8 and SH-10 were found to be statistically significant ($p < 0.01$) (Fig. 4A). Differences between the two pancreatic cancers and between the three colonic cancers were also statistically significant ($p < 0.01$) (Fig. 4B).

DISCUSSION

It is generally considered that increased protein and nucleic acid synthesis and glycolysis are metabolic characteristics of cancer cells (3). In a series of studies using rat hepatomas, it has been shown that there is an increase in amino acid and nucleic acid anabolism as well as glycolysis

TABLE 1
Tissue Distribution of ¹⁸FDG in Nude Mice

Tumor name	Histological subclassification	Minutes*	No. of mice	Blood	Tumor	Heart	Liver	Kidney	Muscle
Gastric cancer H-111	Well differentiated adenocarcinoma	10	6	2.3 ± 0.5 [†]	3.6 ± 1.5	22.7 ± 9.0	2.5 ± 0.3	3.3 ± 0.3	2.4 ± 0.8
		30	6	0.59 ± 0.06	2.4 ± 0.7	32.1 ± 11.6	1.2 ± 0.5	1.7 ± 0.5	1.9 ± 0.9
		60	6	0.37 ± 0.03	2.1 ± 0.2	47.0 ± 11.6	1.1 ± 0.7	1.6 ± 0.3	2.3 ± 0.8
		90	5	0.35 ± 0.03	2.2 ± 0.4	24.1 ± 4.7	0.7 ± 0.1	0.8 ± 0.1	1.2 ± 0.2
NS-8	Moderately differentiated adenocarcinoma	10	6	3.6 ± 0.8	4.4 ± 0.3	6.0 ± 2.7	3.6 ± 0.5	4.7 ± 0.5	2.4 ± 0.4
		30	6	1.1 ± 0.1	3.4 ± 0.5	7.3 ± 1.8	1.1 ± 0.5	1.5 ± 0.6	2.3 ± 0.6
		60	6	0.55 ± 0.04	3.9 ± 0.6	7.7 ± 2.3	1.2 ± 0.4	1.1 ± 0.03	2.0 ± 0.9
		90	6	0.50 ± 0.05	3.8 ± 0.8	6.4 ± 4.1	1.2 ± 0.4	1.2 ± 0.3	1.8 ± 0.7
SC-6-JCK	Poorly differentiated adenocarcinoma	30	6	1.6 ± 0.9	5.8 ± 2.9	47.5 ± 17.4	4.7 ± 2.3	4.6 ± 2.2	1.6 ± 1.0
		60	5	0.57 ± 0.04	5.5 ± 1.9	45.8 ± 8.8	2.0 ± 1.3	1.5 ± 0.3	2.0 ± 0.8
		90	5	0.51 ± 0.09	4.9 ± 1.8	48.5 ± 7.7	2.6 ± 1.3	1.8 ± 1.2	1.2 ± 0.7
SH-10	Undifferentiated carcinoma	10	5	2.4 ± 0.5	4.0 ± 0.6	18.1 ± 11.4	2.5 ± 0.5	3.0 ± 1.6	1.0 ± 0.2
		30	5	0.91 ± 0.19	6.1 ± 1.5	50.3 ± 24.0	2.0 ± 0.5	2.7 ± 0.5	1.0 ± 0.6
		60	6	0.63 ± 0.07	6.4 ± 1.5	37.0 ± 22.7	1.6 ± 0.3	1.7 ± 0.3	1.1 ± 0.5
		90	6	0.48 ± 0.08	6.7 ± 1.9	40.5 ± 27.2	1.3 ± 0.8	1.6 ± 0.8	1.2 ± 0.6
Pancreatic cancer PAN-1-RITC	Well differentiated adenocarcinoma	10	6	3.5 ± 1.4	3.8 ± 0.6	27.9 ± 10.5	5.1 ± 2.2	5.1 ± 1.2	1.1 ± 0.4
		30	6	1.2 ± 0.3	3.7 ± 0.3	26.0 ± 10.4	2.5 ± 0.7	2.4 ± 0.2	1.6 ± 0.7
		60	6	0.63 ± 0.04	3.3 ± 0.5	17.8 ± 6.3	3.2 ± 1.5	1.5 ± 0.2	2.0 ± 0.8
		90	6	0.60 ± 0.06	3.3 ± 0.5	12.8 ± 3.9	1.5 ± 0.2	1.3 ± 0.1	2.2 ± 0.5
PAN-2-RITC	Poorly differentiated adenocarcinoma	10	6	5.3 ± 0.9	5.3 ± 0.7	12.7 ± 3.1	5.3 ± 0.5	6.9 ± 1.0	2.6 ± 1.1
		30	6	2.2 ± 0.3	5.0 ± 0.6	7.5 ± 1.3	2.8 ± 0.3	3.3 ± 0.4	2.2 ± 1.1
		60	6	0.80 ± 0.21	4.8 ± 1.0	11.4 ± 5.9	1.9 ± 0.3	1.9 ± 0.2	2.1 ± 1.1
		90	6	0.71 ± 0.31	4.5 ± 0.6	11.0 ± 3.9	1.7 ± 0.4	1.6 ± 0.2	3.0 ± 1.2
Colonic cancer WIDr	Well differentiated adenocarcinoma	10	6	4.2 ± 1.3	5.6 ± 0.6	18.7 ± 8.3	4.0 ± 1.1	5.0 ± 1.3	1.5 ± 0.4
		30	6	1.2 ± 0.2	4.9 ± 0.8	11.2 ± 4.2	1.7 ± 0.3	2.1 ± 0.5	1.6 ± 0.6
		60	6	0.91 ± 0.15	4.3 ± 0.5	16.3 ± 6.3	1.5 ± 0.2	1.7 ± 0.2	2.3 ± 0.6
		90	5	0.64 ± 0.19	4.0 ± 0.7	12.0 ± 2.9	0.9 ± 0.2	1.2 ± 0.4	1.7 ± 0.6
SCC	Moderately differentiated adenocarcinoma	10	6	4.8 ± 0.6	4.8 ± 0.7	15.9 ± 7.0	5.4 ± 0.9	6.6 ± 0.8	2.7 ± 1.2
		30	6	1.8 ± 0.2	5.6 ± 0.8	14.6 ± 4.7	2.1 ± 0.2	2.8 ± 0.2	2.6 ± 1.0
		60	6	0.85 ± 0.12	5.4 ± 0.5	15.8 ± 5.7	1.3 ± 0.2	1.7 ± 0.2	1.8 ± 0.8
		90	6	0.87 ± 0.13	6.0 ± 0.5	12.1 ± 4.6	1.5 ± 0.2	1.8 ± 0.4	2.1 ± 1.4
CoLo	Poorly differentiated adenocarcinoma	30	6	1.8 ± 0.3	6.0 ± 1.4	15.7 ± 4.1	2.4 ± 0.6	3.2 ± 0.4	3.8 ± 1.3
		60	6	1.0 ± 0.1	7.0 ± 0.7	14.6 ± 6.8	1.5 ± 0.1	2.0 ± 0.3	2.7 ± 1.0
		90	6	0.78 ± 0.03	6.9 ± 0.5	19.5 ± 7.7	1.3 ± 0.1	1.6 ± 0.1	2.7 ± 1.0

*Time (minutes) after the injection of ¹⁸FDG.

[†]Mean ± s.d. (%ID/g tissue).

Values are expressed as %ID/g of tissue.

in parallel with increments in growth rate and loss of histological differentiation (3, 4, 19–23, 34, 35).

The development of PET and ¹⁸FDG as a tracer for glycolysis provides a noninvasive methodology that can give quantitative information on regional glycolytic processes (7,8). The success of tumor imaging with ¹⁸FDG-PET is based on preferential accumulation of ¹⁸FDG in tumors. Some experiments using tumors from animals have confirmed that ¹⁸FDG accumulates in malignant tumors (16–18). Som et al. (16) showed early and high uptake of ¹⁸FDG in a variety of transplanted and spontaneous tumors in mice, rats, hamsters, rabbits and a dog. Fukuda et al. (17) demonstrated a high uptake of ¹⁸FDG in a transplanted ascitic hepatoma (AH109A) in rats. However, there are few studies which used human cancer models.

The human tumor/nude mice system developed by Regaard and Povlsen allows successful heterotransplantation of human tumors in nude mice with preservation of various

characteristics of the original tumors such as morphology and function (36,37). Wahl et al. (38) reported high uptake of ¹⁸FDG into several human tumors xenografted in nude mice for the following tumor types: Burkitt lymphomas, colon carcinoma, renal carcinoma, bladder carcinoma, choriocarcinoma, ovarian carcinoma, small-cell lung cancer, melanoma and neuroblastoma. In the present study, we also investigated the time course of ¹⁸FDG tissue distributions in nude mice bearing nine human cancers, further comparing ¹⁸FDG tumor uptake with histological grade.

The uptake of ¹⁸FDG by the heart was consistently the highest, but the values demonstrated great differences, especially in the gastric cancer series. Yamada et al. (39) reported that myocardial uptake of ¹⁸FDG was greatly changed by glucose and insulin levels. Our experiments were performed without starving the mice. Whereas, in most cases, ¹⁸FDG was injected around 4–6 p.m. when the

mice had not been eating for half the day, in the gastric cancer series (exception NS-8), ^{18}F FDG was supplied late at night when the mice had already started to eat. Differences in nutritional status at the time of ^{18}F FDG injection might have been the reason for the great differences in observed heart uptake. However, as Yamada et al. (39) have indicated, tumor uptake remains relatively unchanged, irrespective of blood glucose levels and differences in nutritional status are not thought to be an influential condition in comparing ^{18}F FDG tumor uptake. The uptake of ^{18}F FDG by each cancer cell line was considerably higher than the liver, the kidney, the muscle or the blood. This enables us to obtain cancer images contrasted with the surrounding organs and is a factor of obvious benefit for detecting cancers located in the abdomen (17).

We believe that the ^{18}F FDG-PET technique has two advantages. First, it reflects tumor viability (40) and can thus be used to monitor anticancer therapy (41, 42). Second, as indicated by the present results and previous studies (3, 4, 19–23), it could be used for diagnosing the malignancy grade of individual cancers.

Weber et al. (19) showed that the glycolytic rate was not appreciably higher in well differentiated, slowly growing Morris hepatoma than in normal liver and was much lower than in poorly differentiated rapidly growing Novikoff hepatomas. Weinhouse (3) and others (20–23) further reported that slowly growing highly differentiated hepatomas exhibit the same pattern of low hexokinase and high glucokinase values as normal adult liver, whereas fast-growing, poorly differentiated hepatomas had a marked increase in hexokinase activity and a virtual disappearance of glucokinase activity. These observations support a positive correlation between the degree of glycolysis and tumor malignancy grading, as reflected in growth rate and degree of histologic differentiation.

The development of ^{18}F FDG-PET (10–15) and scintigra-

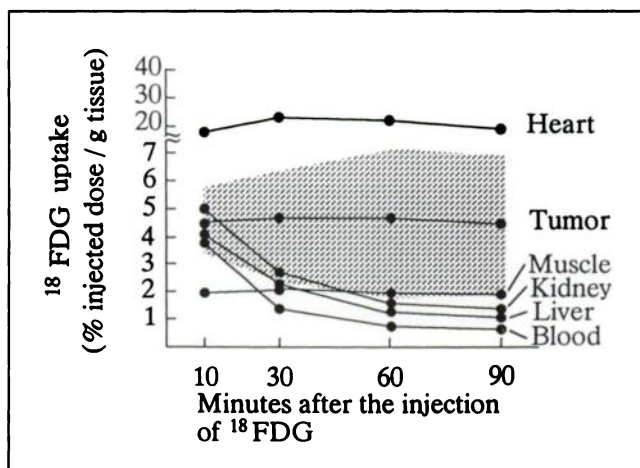


FIGURE 3. Fluorine-18-FDG tissue distribution in nude mice bearing human cancers. Each dot indicates the mean uptake value of normal tissue and nine tumor cell lines of nude mice used in all tissue distribution studies. All tumor uptake values are shown in the shadowed area in the figure.

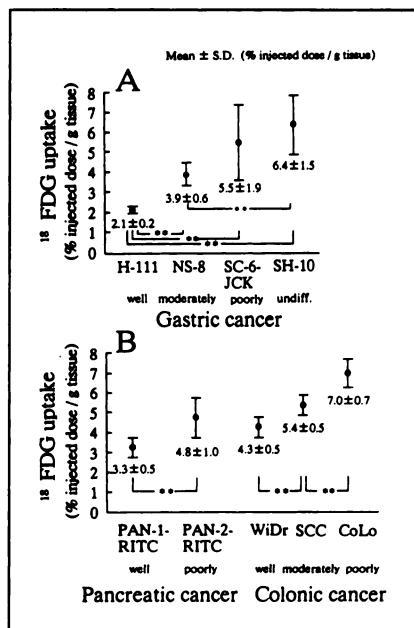


FIGURE 4. Tumor uptake at 60 min after administration of ^{18}F FDG. (A) Gastric cancers and (B) pancreatic and colonic cancers. Fluorine-18-FDG uptake values are increased linearly with degree of differentiation in each organ. Statistical analysis was obtained with the Student's t-test. * $p < 0.05$; ** $p < 0.01$. Bars are \pm s.d.

phy (43) has made it possible to quantitate glycolytic processes in normal as well as in pathologic conditions. Di Chiro et al. (10) studied 100 cases of cerebral gliomas with ^{18}F FDG-PET and reported a strong correlation between tumor grade and glycolytic rate. They reported that not only was there a clear separation of high-grade (III and IV) from low-grade (I and II) tumors, but there was even a statistically significant difference in ^{18}F FDG uptake between grades III and IV. They also reported that glucose utilization rates assessed with ^{18}F FDG-PET appeared to be at least as reliable as histologic classification and other proposed criteria for predicting the behavior and recurrence of intracranial meningiomas (11).

Furthermore, Patronas et al. (12) described PET results for patients with high-grade gliomas that correlated better with length of survival than did histologic subclassification (grade III versus grade IV). Kern et al. (13) studied five patients with musculoskeletal extremity tumors using ^{18}F FDG-PET and also showed a good correlation between histopathologic grading and glucose utilization rates measured from ^{18}F FDG-PET images. Adler et al. (14) similarly studied five patients with liposarcomas of the thigh using ^{18}F FDG-PET and found that the histological grade of malignancy was closely correlated with the uptake ratio for ^{18}F FDG. On the other hand, Nolop et al. (15) reported that there was little correlation between tumor type and rate of ^{18}F FDG uptake in 12 lung cancer patients. They mentioned that lung tumors might in fact differ from other tumors in enzymatic or membrane transport changes accompanying differentiation loss, but that the findings might equally be explained by the smallness of the histologic samples and heterogeneous metabolic activity within tumors.

Our present study on the correlation between the degree of glycolysis and degree of histologic differentiation using human tumor xenografts demonstrated ^{18}F FDG uptake to be

increased with the grade of differentiation in carcinomas from the stomach, pancreas and colon. Because the tumors may not retain their morphological properties during successively repeated transplants, all excised tumors were examined by pathological specialists. The possibility that stromal tissues originating from mice played a differential role could be ruled out by measuring tumor parenchyma-to-stroma volume ratios in the nine cancer types used in our study.

Minn et al., who studied 13 patients with malignant head and neck tumors using ^{18}F FDG scintigraphy, reported that ^{18}F FDG accumulation did not correlate with tumor histologic grade but rather was associated with proliferative activity, as measured by DNA flow cytometry (43). Although ^{18}F FDG uptake of rapidly growing colonic and poorly and moderately differentiated adenocarcinomas were higher than in slowly growing well differentiated tumors, the fact that marked variations uptake were observed for gastric and pancreatic cancers of similar growth rates suggests that the degree of glycolysis and ^{18}F FDG accumulation in tumors may correlate with loss of histologic differentiation independent of proliferative status. Higashi et al. recently reported that ^{18}F FDG uptake did not relate to the proliferative activity of cancer cells but to the number of viable tumor cells (44). The space occupied by glands in highly differentiated cancers is greater than that in poorly differentiated counterparts and the number of viable cells in the former per unit volume is therefore smaller than in the latter. The difference in ^{18}F FDG tumor uptake between lesions with varying histologic grade but equal growth rate may be caused by differences in viable cell numbers.

We have used only nine human cell lines and further studies with more tumor types are warranted. It must be emphasized that internal tumors are often histologically heterogeneous and contain various volumes of stromal tissues and necrotic areas, so our results may not be directly applicable to clinical ^{18}F FDG-PET tumor images. The results suggest, however, that this approach warrants further investigation in both clinical and experimental settings.

ACKNOWLEDGMENTS

We are grateful to Drs. Nakatani, Nitani, Saeki and Takahashi for supplying the human cancer strains. We also thank Dr. Fukuda for his helpful comments and the staff of the Cyclotron Radioisotope Center, particularly Drs. Ishiwata, Iwata and Takahashi, for their assistance.

This study was supported in part by Grants-in-Aid for Cancer Research (1-9 and 62S-1) from the Ministry of Health and Welfare and for Scientific Research (No. 01570347) from the Ministry of Education, Science and Culture. This paper is based on work performed for a doctoral dissertation at Tohoku University.

REFERENCES

1. Warburg O. *The metabolism of tumors*. London: Arnold Constable; 1930: 75-327.
2. Warburg O. On the origin of cancer cells. *Science* 1956;123:309-314.
3. Weinhouse S. Glycolysis, respiration, and anomalous gene expression in

- experimental hepatomas: G.H.A. Clowes memorial lecture. *Cancer Res* 1972;32:2007-2016.
4. Weber G. Enzymology of cancer cells. *N Engl J Med* 1977;296:486-493, 541-551.
5. Bessel EM, Foster AB, Westerwood JH. The use of deoxy-fluoro-D-glucopyranoses and related compounds in a study of yeast hexokinase specificity. *Biochem J* 1972;128:199-204.
6. Reivich M, Kuhl D, Wolf A, et al. The [^{18}F]fluorodeoxyglucose method for the measurement of local cerebral glucose utilization in man. *Circ Res* 1979;44:127-137.
7. Gallagher BM, Fowler JS, Gutterson NI, MacGregor RR, Wan CN, Wolf AP. Metabolic trapping as a principle of radiopharmaceutical design: some factors responsible for the biodistribution of [^{18}F]2-deoxy-2-fluoro-D-glucose. *J Nucl Med* 1978;19:1154-1161.
8. Ratib O, Phelps ME, Huang SC, Henze E, Selin CE, Schelbert HR. Positron tomography with deoxyglucose for estimating local myocardial glucose metabolism. *J Nucl Med* 1982;23:577-586.
9. Hoffman EJ, Phelps ME, Mullani NA, Higgins CS, Ter-Pogossian MM. Design and performance characteristics of a whole-body positron transaxial tomograph. *J Nucl Med* 1976;17:493-502.
10. Di-Chiro G. Positron emission tomography using [^{18}F]fluorodeoxyglucose in brain tumors. A powerful diagnostic and prognostic tool. *Invest Radiol* 1986;22:360-371.
11. Di-Chiro G, Hatazawa J, Katz DA, Rizzoli HV, De-Michele DJ. Glucose utilization by intracranial meningiomas as an index of tumor aggressivity and probability of recurrence: a PET study. *Radiology* 1987;164:521-526.
12. Patronas NJ, Di-Chiro G, Kufta C, et al. Prediction of survival in glioma patients by means of positron emission tomography. *J Neurosurg* 1985;62: 816-822.
13. Kern KA, Brunetti A, Norton JA, et al. Metabolic imaging of human extremity musculoskeletal tumors by PET. *J Nucl Med* 1988;29:181-186.
14. Adler LP, Blair HF, Williams RP, et al. Grading liposarcomas with PET using [^{18}F]FDG. *J Comput Assist Tomogr* 1990;14:960-962.
15. Nolop KB, Rhodes CG, Brudin LH, et al. Glucose utilization in vivo by human pulmonary neoplasms. *Cancer* 1987;60:2682-2689.
16. Som P, Atkins HL, Bandyopadhyay D, et al. Fluorinated glucose analog, 2-fluoro-2-deoxy-D-glucose (F-18): nontoxic tracer for rapid tumor detection. *J Nucl Med* 1980;21:670-675.
17. Fukuda H, Matsuzawa T, Abe Y, et al. Experimental study for cancer diagnosis with positron-labeled fluorinated glucose analogs: [^{18}F]2-fluoro-2-deoxy-D-mannose: a new tracer for cancer detection. *Eur J Nucl Med* 1982;7:294-297.
18. Larson SM, Weiden PL, Grunbaum Z, et al. Positron imaging feasibility studies. II: characteristics of 2-deoxyglucose uptake in rodent and canine neoplasms: concise communication. *J Nucl Med* 1981;22:875-879.
19. Weber G, Banerjee G, Morris HP. Comparative biochemistry of hepatomas I. Carbohydrate enzymes in Morris hepatoma 5123. *Cancer Res* 1961;21: 933-937.
20. Elwood JC, Lin YC, Cristofalo VJ, Weinhouse S, Morris HP. Glucose utilization in homogenates of the Morris hepatoma 5123 and related tumors. *Cancer Res* 1963;23:906-913.
21. Sweeny MJ, Ashmore J, Morris HP, Weber G. Comparative biochemistry of hepatomas IV. Isotope studies of glucose and fructose metabolism in liver tumors of different growth rates. *Cancer Res* 1963;23:995-1002.
22. Lo CH, Cristofalo VJ, Morris HP, Weinhouse S. Studies on respiration and glycolysis in transplanted hepatic tumors of the rat. *Cancer Res* 1968;28:1-10.
23. Knox WE, Jamdar SC, Davis PA. Hexokinase, differentiation and growth rates of transplanted rat tumors. *Cancer Res* 1970;30:2240-2244.
24. Kondo T, Imaizumi M, Taguchi T, et al. A model for sensitivity determination of anticancer agents against human cancer using nude mice. *Jpn J Cancer Chemother* 1987;14:680-686 (in Japanese).
25. Nakatani K, Miyagi N, Ezaki T, et al. Heterotransplantation of human gastric carcinoma into nude mice. 9. Transplantation of cell suspension of serially transplanted human gastric cancer in subcutaneous tissue into the peritoneal cavity of nude mice. *J Jpn Soc Cancer Ther* 1984;19:88-94 (in Japanese).
26. Sato H. List of transplantable tumors maintained in Japan. *Nippon de iisareteiru kaisyokuseisyuyoukaku itiranhyou*. 1987;37-42 (in Japanese).
27. Ueno M, Takahashi Y, Akimoto R, Mai M. Heterotransplantation of human malignant tumor into nude mice. Transplantability and its relation with several histological incidents. *Journal of Society of Hokuriku Surgery Hokuriku gekagakkai zasshi* 1984;3:7-11 (in Japanese).
28. Noguchi P, Wallace R, Johnson J, et al. Characterization of WiDr: a human colon carcinoma cell line. *In Vitro* 1979;15:401-408.

29. Semple TU, Quinn LA, Woods LK, Moore GE. Tumor and lymphoid cell lines from a patient with carcinoma of the colon for a cytotoxicity model. *Cancer Res* 1978;38:1345-1355.
30. Kikuchi H, Asamura M, Gamoh M, et al. Comparison of subrenal capsule and subcutaneous assay using nude mouse on pancreatic cancer. *Jpn J Cancer Chemother* 1991;18:305-308.
31. Shiue CY, Salvadori PA, Wolf AP, Fowler JS, MacGregor RR. A new improved synthesis of 2-deoxy-2-[¹⁸F]fluoro-D-glucose from ¹⁸F-labeled acetyl hypofluorite. *J Nucl Med* 1982;23:899-903.
32. Geran RI, Greenberg NH, Macdonald MM, Schumacher AM, Abbott BJ. Protocols for screening chemical agents and natural products against animal tumors and other biological systems. *Cancer Chemother Res* 1972;3:51-61.
33. Weidel ER. *Stereological method*. London: Academic Press, 1980, 55-81.
34. Wagle SR, Morris HP, Weber G. Comparative biochemistry of hepatomas. V. Studies on amino acid incorporation in liver tumors of different growth rates. *Cancer Res* 1963;23:1003-1007.
35. Lea MA, Morris HP, Weber G. Comparative biochemistry of hepatomas. VI. Thymidine incorporation into DNA as a measure of hepatoma growth rate. *Cancer Res* 1966;26:465-469.
36. Rygaard J, Povlsen CO. Heterotransplantation of a human malignant tumor to "nude" mice. *Acta Path Microbiol Scand* 1969;77:758-760.
37. Povlsen CO, Rygaard J. Heterotransplantation of human adenocarcinomas of the colon and rectum to the mouse mutant nude. A study of nine consecutive transplantations. *Acta Path Microbiol Scand* 1971;79:159-169.
38. Wahl RL, Hutchins GD, Buchsbaum DJ, Liebert M, Grossman HB, Fisher S. Fluorine-18-2-deoxy-2-fluoro-D-glucose uptake into human tumor xenografts: feasibility studies for cancer imaging with positron-emission tomography. *Cancer* 1991;67:1544-1550.
39. Yamada K, Endo S, Fukuda H, et al. Experimental studies on myocardial glucose metabolism of rats with ¹⁸F-2-fluoro-2-deoxy-D-glucose. *Eur J Nucl Med* 1985;10:341-345.
40. Iosilevsky G, Front D, Bettman L, Hardoff R, Ben-Arieh Y. Uptake of gallium-67 citrate and [2-³H]deoxyglucose in the tumor model, following chemotherapy and radiotherapy. *J Nucl Med* 1985;26:278-282.
41. Takahashi H, Yamaguchi K, Wakui A, et al. New approach to clinical evaluation of cancer chemotherapy using positron emission tomography with ¹⁸FDG (2-deoxy-2-[¹⁸F]fluoro-D-glucose). *Sci Rep Res Inst Tohoku Univ* 1986;33:38-43.
42. Valk PE, Budinger TF, Levin VA, Silver P, Gutin PH, Doyle WK. PET of malignant cerebral tumors after interstitial brachytherapy. Demonstration of metabolic activity and correlation with clinical outcome. *J Neurosurg* 1988;69:830-838.
43. Minn H, Joensuu H, Ahonen A, Klemi P. Fluorodeoxyglucose imaging: a method to assess the proliferative activity of human cancer in vivo. Comparison with DNA flow cytometry in head and neck tumors. *Cancer* 1988; 61:1776-1781.
44. Higashi K, Clavo AC, Wahl RL. Does FDG uptake measure proliferative activity of human cancer cells? In vitro comparison with DNA flow cytometry and tritiated thymidine uptake. *J Nucl Med* 1993;34:414-419.